

# Calculation of vibrational excitation cross-sections in resonant electron-molecule scattering using the time-dependent wave packet (TDWP) approach with application to the ${}^2\Pi$ $\text{CO}^-$ shape resonance

RAMAN KUMAR SINGH,<sup>1</sup> MANABENDRA SARMA,<sup>1</sup> ANKIT JAIN,<sup>1</sup>  
SATRAJIT ADHIKARI<sup>1,2</sup> and MANOJ K MISHRA<sup>1,\*</sup>

<sup>1</sup>Department of Chemistry, Indian Institute of Technology Bombay, Powai, Mumbai 400 076

<sup>2</sup>Department of Chemistry, Indian Institute of Technology Guwahati, North Guwahati 781 039

e-mail: mmishra@iitb.ac.in

MS received 5 June 2007; accepted 7 July 2007

**Abstract.** Results from application of a new implementation of the time-dependent wave packet (TDWP) approach to the calculation of vibrational excitation cross-sections in resonant e-CO scattering are presented to examine its applicability in the treatment of e-molecule resonances. The results show that the SCF level local complex potential (LCP) in conjunction with the TDWP approach can reproduce experimental features quite satisfactorily.

**Keywords.** Electron scattering; shape resonance; vibrational excitation; time dependent wave packet (TDWP); local complex potential.

## 1. Introduction

The shape resonances in low energy scattering of electrons off diatomic targets (A) are believed to result from formation of a compound anionic state ( $A^-$ ) whereupon the nuclei start to move in the local complex potential (LCP)  $W(R) = E_A - (R) - \frac{1}{2}\Gamma_A - (R)$  of the anion. For resonant anions with lifetime in excess of the vibrational period of  $A^-$ , the visiting electron is re-emitted after the anion has completed at least one vibration, the nuclear wave function for  $A^-$  exhibits a reflection from the right turning point, and there is vibrational structure in the resonant scattering cross-sections even for the lowest vibrational excitation of the target.<sup>1–5</sup> The pronounced vibrational structure accompanying the formation of  ${}^2\Pi_g\text{N}_2^-$  shape resonance in e- $\text{N}_2$  scattering is a much studied example<sup>1–12</sup> of enduring interest and the decay mechanism is popularly labeled as the *boomerang* model<sup>3,4</sup> because of the return of the anionic nuclear wave packet from the right turning point. If the lifetime of the resonant anionic state  $A^-$  is smaller than its vibrational period, then the anionic wave function decays before it can rebound from the right turning

point of  $A^-$  and for the lowest vibrational excitations, the resonance scattering cross-sections only show broad smooth peaks as a function of energy.<sup>1–5,12–22</sup> Vibrational structure in this case occurs only for higher level excitations of the target A since the larger inter-nuclear span of higher vibrational states permits an increase of the traversal/decay time and thereby sampling of interference structure between the A and  $A^-$  vibrational levels.<sup>3,4,12</sup> The role of the impinging electron in this case is to provide an impulse for quick decay of the compound anion and the  ${}^2\Sigma_u^+\text{H}_2^-$  shape resonance in e- $\text{H}_2$  scattering provides an example of the *impulse* model<sup>3,4,12,13</sup> for resonance decay.

We have recently implemented a cross-correlation based TDWP approach<sup>12</sup> where simple local complex potentials (LCP) for  ${}^2\Pi_g\text{N}_2^-$  and  ${}^2\Sigma_u^+\text{H}_2^-$  have provided very reasonable agreement with experimental vibrational excitation cross-sections for both these systems. The carbon monoxide molecule is isoelectronic with  $\text{N}_2$  but does not have a centre of symmetry, whereby, the parity concerns which preclude the participation of  $\ell = 1(u)$  partial wave in the description of the gerade  ${}^2\Pi_g\text{N}_2^-$  are not present for  $\text{CO}^-$  and the additional decay channel not accessible for  $\text{N}_2^-$  decay becomes available whereby the lifetime of  $\text{CO}^-$  is less than that of  $\text{N}_2$  but larger than that of  $\text{H}_2^-$  and dy-

\*For correspondence

nomical details of the e-CO scattering<sup>4,5,23–26</sup> are those intermediate between e-N<sub>2</sub> and e-H<sub>2</sub> scattering.

Application of our newly developed TDWP implementation<sup>12</sup> using simple LCPs for CO<sup>-</sup> is therefore an obvious test of its effectiveness and it is our purpose in this paper to provide initial results from TDWP calculation of vibrational excitation cross-sections in the e-CO scattering using a simple UHF LCP for this system.

A skeletal outline of the methodological details is presented in §2 and the TDWP results are presented and discussed in §3. A brief outline of the main results concludes this paper.

## 2. Method

As outlined by McCurdy and Turner,<sup>11</sup> the transition matrix elements for vibrational excitation cross-section in the time-dependent formulation may be obtained as Fourier transform of the cross correlation function<sup>27</sup>  $\langle \phi_{v_f}(R) | \psi_{v_i}(R, t) \rangle$  i.e.

$$T_{v_f, v_i}(E) = -\frac{i}{\hbar} \int_0^{\infty} e^{iEt/\hbar} \langle \phi_{v_f}(R) | \psi_{v_i}(t) \rangle dt, \quad (1)$$

where the time dependent function  $\psi_{v_i}(R, t)$  represents the time evolution of the initial target vibrational state  $\phi_{v_i}(R)$  under the influence of the resonance anionic Hamiltonian  $H_{A^-}$  i.e.

$$\psi_{v_i}(R, t) = e^{-iH_{A^-}(R)t/\hbar} \phi_{v_i}(R) \quad (2)$$

$$\text{with } H_{A^-}(R) = -\frac{\hbar^2}{2\mu_{A^-}} \nabla^2 + W(R); \quad (3)$$

and  $W(R) = E_{A^-}(R) - i/2\Gamma_{A^-}(R)$ , is the complex local potential governing the nuclear motion of the metastable A<sup>-</sup>.  $E_{A^-}(R)$  and  $E_{A^-}(R)$  have generally been parameterized<sup>3,6,13,24</sup> or approximated with simple harmonic potentials<sup>6</sup> but we have computed the potential energy (PE) curves  $E_{\text{CO}}(R)$  and  $E_{\text{CO}^-}(R)$  at various levels of accuracy (UHF, MP2, QCID, etc.) and in this implementation have chosen to use the basic UHF potentials (figure 1a) because this provides the best fit to the requirement that the width function  $\Gamma_{A^-}(R)$  as given by the Blatt and Weisskopf prescription<sup>28</sup>

$$\Gamma(R) = \Gamma(R_0) \frac{\kappa(R)}{\kappa(R_0)} \frac{v_2[\kappa(R)\rho]}{v_2[\kappa(R_0)\rho]}, \quad (4)$$

goes to zero at the crossing point of  $E_{\text{CO}}(R)$  and  $E_{\text{CO}^-}(R)$ . PE curves obtained using MP2 and QCID did not fulfill this requirement and we have not pushed this matter further because of the difficulties in balanced correlation for both the neutral target and its anion at these levels and the preliminary demonstrative nature of the initial calculations presented here. In (4)

$$v_2(x) \equiv x^4/(9 + 3x^2 + x^4), \quad \text{and}$$

$$\kappa(R) = (2m/h)^{1/2} [E_{A^-}(R) - E_A(R)]^{1/2}, \quad (5)$$

$R_0$  is the equilibrium separation of the CO<sup>-</sup> nuclei and  $\rho$  is the distance from centre of mass of the tar-

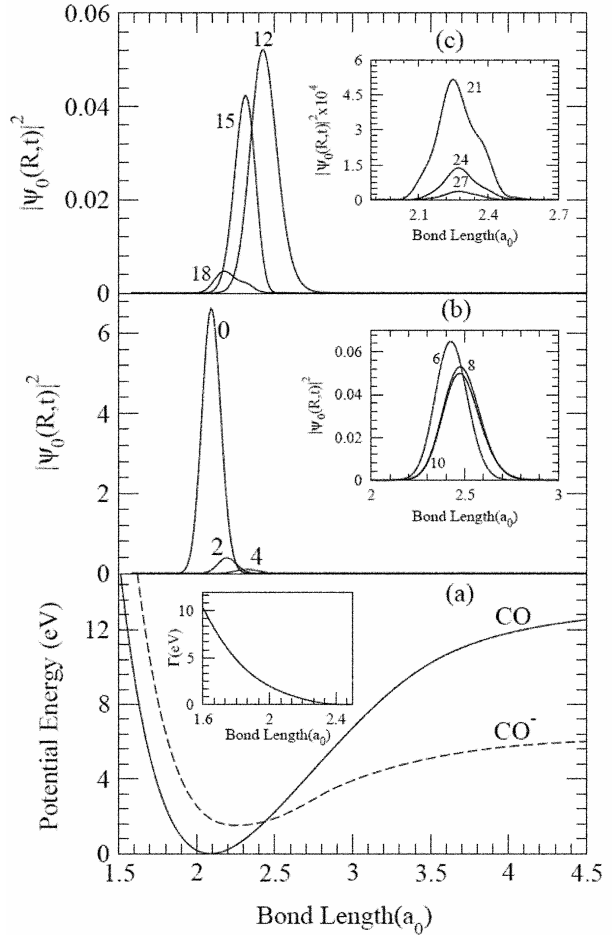


**Figure 1.** Potential energy curve for CO and the real part [ $E_{\text{CO}^-}(R)$ ] of the local complex potential [ $W_{\text{CO}^-}(R)$ ] are plotted in (a). The imaginary part of  $W_{\text{CO}^-}(R)$  [width  $\Gamma_{\text{CO}^-}(R)$ ] is provided as inset in (a). Time evolution of ground state wave function  $\phi_0(R)$  of CO under the influence of the CO<sup>-</sup> Hamiltonian from 0 to 10 fs is presented in 1b and from 12 to 27 fs in 1c.

get molecule beyond which electron is considered to be free.  $\rho$  has been fixed at 1.6 Å as per the Dubé and Herzberg<sup>6</sup> prescription adopted by Zubek and Szmytkowski<sup>24</sup> for this system. Finally, the vibrational excitation cross-section  $\sigma_{v_f \leftarrow v_i}(E)$  may then be obtained from<sup>11</sup>

$$\sigma_{v_f \leftarrow v_i}(E) = \frac{8\pi^3}{k_i^2} |T_{v_f, v_i}(E)|^2, \quad (6)$$

where  $k_i$  represents momentum of the incident electron.

The vibrational target wave functions  $\phi_{v_i}(R)$  and  $\phi_{v_f}(R)$  of CO were obtained by applying Fourier grid Hamiltonian (FGH) approach<sup>29,30</sup> to  $E_{\text{CO}}(R)$ . In

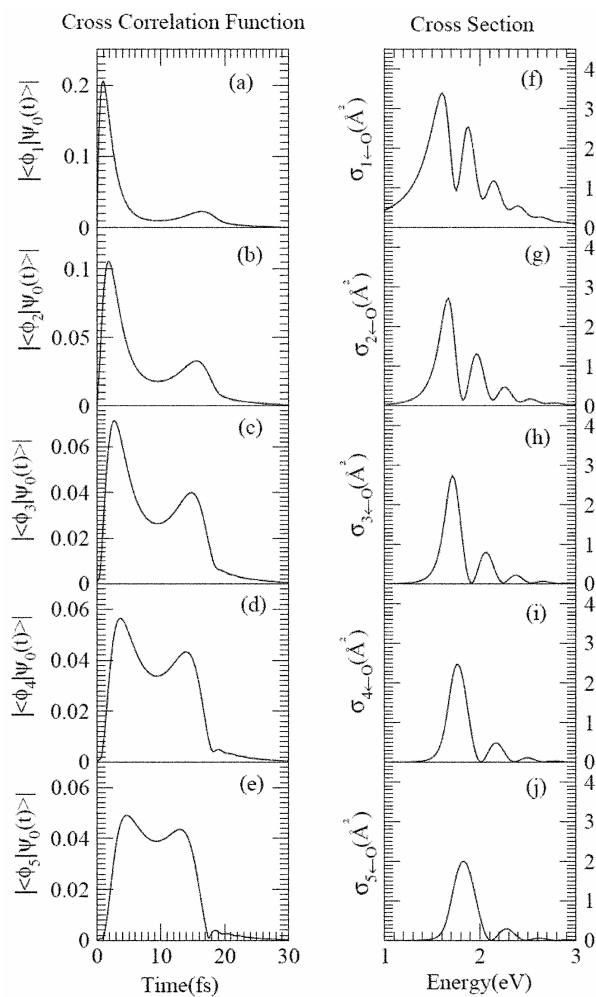


**Figure 2.** Calculated cross correlation functions  $\langle \phi_n | \psi_0(t) \rangle$  [(a)–(e)] and corresponding vibrational excitation cross sections  $\sigma_{n \leftarrow 0}(E)$  [(f)–(j)] for e-CO scattering.

time evolution of the ground vibrational state  $\phi_0(R)$  of the CO target under the influence of CO Hamiltonian (2, 3) the effect of kinetic energy operator is evaluated using 1-D Fast Fourier Transform (FFT)<sup>31</sup> and time evolution of  $\phi_0^{\text{CO}}(R)$  under the influence of  $H_{\text{CO}}(R)$  is performed using Lanczos transform.<sup>32</sup>

### 3. Results and discussion

The UHF PE curves for CO and  $\text{CO}^-$  are presented in figure 1a and the width function  $\Gamma_{\text{CO}^-}(R)$  calculated using (4) and (5) is plotted in the inset of figure 1a. These compare reasonably well with those utilized by Zubek and Szmytkowski<sup>24</sup> and Morgan.<sup>26</sup> Time evolution of the CO ground vibrational state ( $\phi_0$ ) under the influence of  $\text{CO}^-$  Hamiltonian on resonant electron capture by the target CO molecule  $\psi_0(R, t) \equiv e^{-iH_{\text{CO}^-} t/\hbar} \phi_0^{\text{CO}}(R)$  is charted in figures 1b and c. The fast decay of the  $\text{CO}^-$  anion is clearly seen from these plots as also the reflection of the nuclear wave function  $\psi_0(R, t)$  from the right turning point of the  $\text{CO}^-$  PE curve at 15 fs whose peak is to the left of the  $\psi_0(R, t)$  at  $t = 12$  fs. The decay is more or less complete by 21 fs since at this time  $|\psi_0(R, t)|^2 \cdot 10^{-4} |\phi_0(R, t=0)|^2$ . In comparison<sup>12</sup>, the decay of  $|\phi_0(R, t)|^2$  to  $10^{-4} |\phi_0(R, t=0)|^2$  takes 35 fs for  $\text{N}_2$  and only 1 fs for  $\text{H}_2^-$ .

A more quantitative demarcation of the decay pattern is provided by the cross-correlation functions plotted in figures 2a–e. At  $t = 0$ ,  $\psi_0(R, t) = \phi_0(R)$  is orthogonal to  $\phi_n$ ,  $\forall n \neq 0$  and cross-correlation functions therefore start with zero at  $t = 0$  and as  $\psi_0(R, t)$  travels to the right for  $t > 0$  it first increases and then decreases in tune with forward movement accompanied by decay of  $\phi_0(R, t)$  with a second hump resulting from the *boomerang* type return of the wave function to  $R$ -values which provide non-zero overlap between  $\phi_n$  and  $\psi_0(R, t)$ .

Since the inter-nuclear ( $R$ ) span of higher vibrational levels increases with  $n$ , the traversal and consequently the decay time increases for cross-correlation functions  $\langle \phi_n | \psi_0(t) \rangle$  for higher  $n$  (figures 2b–2e). However, larger  $R$  values are sampled at longer time, whereby, with the  $\Gamma(R)$  profile of figure 1a,  $\psi_0(R, t)$  for larger  $R$  keeps decreasing and the higher cross-correlation functions (overlap between  $\phi_n$  and  $\psi_0(R, t)$ ) have smaller magnitude which translates into lower values for the vibrational excitation cross-sections. The  $\sigma_{n \leftarrow 0}(E)$ , therefore, have smaller and lesser number of peaks with increased  $n$  (figures 2f–2j) as observed experimentally.<sup>23,25</sup>

**Table 1.** Peak positions (eV) for calculated and experimental vibrational excitation cross-section  $\sigma_{n\leftarrow 0}(E)$  in e-CO scattering.

Cross-sections	This work			Experimental (ref. 25)		
	Peak 1	Peak 2	Peak 3	Peak 1	Peak 2	Peak 3
$\sigma_{1\leftarrow 0}$	1.61	1.88	2.15	1.58	1.81	2.10
$\sigma_{2\leftarrow 0}$	1.67	1.96	2.25	1.60	1.90	2.25
$\sigma_{3\leftarrow 0}$	1.71	2.07	2.38	1.75	2.05	2.40
$\sigma_{4\leftarrow 0}$	1.77	2.17	2.48	1.80	2.20	2.50
$\sigma_{5\leftarrow 0}$	1.84	2.27	2.61	1.95	2.40	–

The  $\sigma_{n\leftarrow 0}(E)$  peak positions are collected in table 1 and compare favorably with experimental results. The largest deviation from experimental peak position is seen for the 2nd peak of the  $\sigma_{5\leftarrow 0}(E)$  profile which is 2.40 eV (expt.) and 2.27 eV (our calculation) with a < 6% deviation between the experimental and calculated values which for the simple SCF PE curves used here seems quite reasonable. However, it should be mentioned that, the detailed peak structure of the individual  $\sigma_{n\leftarrow 0}(E)$  profiles as calculated by us do not conform completely with either the experimental profiles<sup>23,25</sup> or those calculated using optimized parametric PE curves.<sup>24,26</sup> With the simple SCF level PE curves employed here for reasons discussed earlier, we believe it is not practical to expect complete agreement with all experimental details. It is, however, most gratifying to record that our calculated width (0.20 eV) is identical to the experimental results of Ehrhardt *et al.*<sup>23</sup>

#### 4. Concluding remarks

Our purpose in this paper has been to offer an application of the TDWP approach using standard techniques for obtaining vibrational functions and time evolution to test its applicability using simple local complex potentials in the description of formation and decay of the  ${}^2\Pi\text{CO}^-$  resonance. The results obtained seem to show that our TDWP implementation<sup>12</sup> is quite effective and can provide detailed mechanistic insights into electron–molecule scattering. The evolution of the system can be mapped to any desired level of time resolution and proposed mechanisms investigated in minutest detail.

The PE curves employed in this calculation are non-parametric and no attempt has been made to optimize them to reproduce experimental results. As remarked earlier, the PE curves  $E_{\text{CO}}(R)$  and  $E_{\text{CO}}(R)$  were calculated at MP2 and QCID levels as well but

the  $\Gamma_{\text{CO}}(R)$  calculated from the MP2 and QCID PE curves and Blatt–Weisskopf prescription (4) and (5) do not go to zero at the crossing point between  $E_{\text{CO}}(R)$  and  $E_{\text{CO}}(R)$  as required. For this reason, in this preliminary demonstrative application we have used the SCF PE curves even when dissociation energy and  $\sigma_{n\leftarrow 0}(E)$  calculated from the SCF PE curves show significant deviation from experimental values. It is, therefore, a very pleasant surprise that our results indicate that the experimental structure in vibrational excitation cross-sections in the resonant e-CO scattering do emerge from the simple SCF level local complex potentials utilized by us and the cross correlation functions provide an unequivocal affirmation of the *boomerang* classification for the  ${}^2\Pi\text{CO}^-$  shape resonance.<sup>1–5,23–26</sup> There has been much debate and skepticism about the applicability of LCPs in the treatment of short lifetime resonances,<sup>16–22</sup> but our results show that simple local complex potentials can do justice to almost all features of the vibrational excitation cross-section profiles not only for e-H<sub>2</sub> and e-N<sub>2</sub> scattering<sup>12</sup> but for the e-CO scattering as well.

Unlike in the time independent scattering theory based approaches, where a separate calculation is required for each  $E$ , in the TDWP approach, the energy dependence of all the  $\sigma_{n\leftarrow 0}(E)$  can be obtained from a single calculation. Simultaneous availability of mechanistic details to desired level of temporal/energetic resolution is an additional advantage and this demonstration of reasonable efficacy, we hope, will encourage interest in the use of TDWP approach as an easy to implement alternative for studying the nuclear dynamics of molecular resonances. However, it should be borne in mind that time ( $t$ ) and energy ( $E$ ) being Fourier conjugate variables, the choice of time step size ( $\Delta T$ ) will control the energy resolution ( $\Delta E$ ) of the  $\sigma_{n\leftarrow 0}(E)$  cross-section profile and sub femtosecond time steps will lead to very large  $\Delta E$

wiping out the energy resolution of the cross-section profile and a finer resolution in  $t$  will come at the cost of poor resolution for  $\sigma_{n \leftarrow 0}(E)$  and vice-versa.

### Acknowledgment

This research has been supported by grants from Department of Science and Technology and Board of Research in Nuclear Sciences, India to MKM. MS acknowledges support from Council of Scientific and Industrial Research (CSIR), India. SA acknowledges Department of Science and Technology (DST), Government of India for partial financial support.

### References

1. Herzenberg A 1968 *J. Phys.* **B1** 548
2. Taylor H S 1970 *Adv. Chem. Phys.* **18** 91
3. Birtwistle D T and Herzenberg A 1971 *J. Phys.* **B4** 53
4. Schulz G J 1973 *Rev. Mod. Phys.* **45** 423
5. Jordan K D and Burrow P D 1978 *Acc. Chem. Res.* **11** 341
6. Dubé L and Herzenberg A 1979 *Phys. Rev.* **A20** 194
7. Schneider B I, Dourneuf M L and Lan V K 1979 *Phys. Rev. Lett.* **43** 1926
8. Schneider B I, Dourneuf M L and Burke P G 1979 *J. Phys.* **B12** L365
9. Hazi A U, Rescigno T N and Kurilla M 1981 *Phys. Rev.* **A23** 1089
10. Cederbaum L S and Domcke W 1981 *J. Phys.* **B14** 4665
11. McCurdy C W and Turner J L 1983 *J. Chem. Phys.* **78** 6773
12. Sarma M, Adhikari S and Mishra M K 2007 *J. Chem. Phys.* **126** 044309
13. Bardsley J N and Wadehra J M 1979 *Phys. Rev.* **A20** 1398
14. Berman M, Mündel C and Domcke W and 1985 *Phys. Rev.* **A31** 641
15. Mündel C, Berman M and Domcke W 1985 *Phys. Rev.* **A32** 181
16. Domcke W 1991 *Phys. Rep.* **208** 97
17. Rescigno T N, Elza B K and Lengsfeld B H 1993 *J. Phys.* **B26** L567
18. Narevicius E and Moiseyev N 1998 *Phys. Rev. Lett.* **81** 2221
19. Narevicius E and Moiseyev N 2000 *Phys. Rev. Lett.* **84** 1681
20. Allan M 2005 *J. Phys.* **B38** 3655
21. Houfek K, Rescigno T N and McCurdy C W 2006 *Phys. Rev.* **A73** 032721
22. Horáček J, Čížek M, Houfek K, Kolorenč P and Domcke W 2006 *Phys. Rev.* **A73** 022701 and references therein
23. Ehrhardt H, Langhans L, Linder F and Taylor H S 1968 *Phys. Rev.* **173** 222
24. Zubek M and Szmytkowski C 1977 *J. Phys.* **B10** L27
25. Allan M 1989 *J. Electron. Spectrosc. Rel. Phenomena* **48** 219
26. Morgan L A 1991 *J. Phys.* **B24** 4649
27. Heller E J 1981 *Acc. Chem. Res.* **14** 368
28. Blatt J M and Weisskopf V F 1952 *Theoretical nuclear physics* (New York: Wiley) p. 410
29. Marston C C and Balint-Kurti G G 1989 *J. Chem. Phys.* **91** 3571
30. Balint-Kurti G G, Dixon R N and Marston C C 1992 *Int. Rev. Phys. Chem.* **11** 317
31. Leforestier C, Bisseling R H, Cerjan C, Feit M D, Friesner R, Guldberg A, Hammerich A, Jolicard G, Karrlein W, Meyer H D, Lipkin N, Roncero O and Kosloff R 1991 *J. Comput. Phys.* **94** 59
32. Kosloff D and Kosloff R 1983 *J. Comput. Phys.* **52** 35